

Parabolic equation solution of seismo-acoustics problems involving variations in bathymetry and sediment thickness

Jon M. Collis^{a)} and William L. Siegmann
Rensselaer Polytechnic Institute 110 8th Street, Troy, New York 12180

Finn B. Jensen and Mario Zampolli
NATO Undersea Research Center, 19126 La Spezia, Italy

Elizabeth T. Küsel
Northeastern University 360 Huntington Avenue, Boston, Massachusetts 02115

Michael D. Collins
Naval Research Laboratory, Washington, D.C. 20375

(Received 21 February 2007; revised 21 September 2007; accepted 27 September 2007)

Recent improvements in the parabolic equation method are combined to extend this approach to a larger class of seismo-acoustics problems. The variable rotated parabolic equation [J. Acoust. Soc. Am. **120**, 3534–3538 (2006)] handles a sloping fluid-solid interface at the ocean bottom. The single-scattering solution [J. Acoust. Soc. Am. **121**, 808–813 (2007)] handles range dependence within elastic sediment layers. When these methods are implemented together, the parabolic equation method can be applied to problems involving variations in bathymetry and the thickness of sediment layers. The accuracy of the approach is demonstrated by comparing with finite-element solutions. The approach is applied to a complex scenario in a realistic environment. © 2008 Acoustical Society of America. [DOI: 10.1121/1.2799932]

PACS number(s): 43.30.Ma, 43.30.Dr, 43.30.Gv [RCG]

Pages: 51–55

I. INTRODUCTION

The parabolic equation method is a powerful approach for solving range-dependent propagation problems (i.e., problems in laterally varying media) in ocean acoustics.¹ Since many sediments support shear waves, the development of the elastic parabolic equation^{2–5} has been a topic of great interest. In recent years, there has been a focus on improving accuracy for range-dependent seismo-acoustics problems. The introduction of the (u_r, w) formulation,⁶ where u_r is the range derivative of the horizontal displacement and w is the vertical displacement, has led to progress in this area. An improved single-scattering solution in the (u_r, w) formulation accurately handles range dependence within purely elastic media.⁷ An improved rotated parabolic equation solution accurately handles fluid-solid interfaces of variable slope.⁸ In this paper, we combine these approaches to obtain parabolic equation solutions of problems involving sloping ocean bottoms and varying sediment thickness. We demonstrate the accuracy of the approach by making comparisons with finite-element solutions. We also apply the approach to a model problem based on a complex environment off the New Jersey coast.⁹ The approach is discussed in Sec. II and applied to examples in Sec. III.

II. PARABOLIC EQUATION SOLUTION

We describe the parabolic equation solution in cylindrical coordinates, where the range r is the horizontal distance

from a source and z is the depth below the ocean surface. We work in the far field and remove the cylindrical spreading factor $r^{-1/2}$ from the solution. The parabolic equation method is based on the factorization of the operator in the elliptic wave equation into a product of operators that correspond to outgoing and incoming energy. These factors give rise to the parabolic wave equations⁷

$$\frac{\partial}{\partial r} \begin{pmatrix} u_r \\ w \end{pmatrix} = \pm i(L^{-1}M)^{1/2} \begin{pmatrix} u_r \\ w \end{pmatrix}, \quad (1)$$

where L and M are matrices containing depth operators, the plus sign corresponds to outgoing waves, and the negative sign corresponds to incoming waves. The outgoing wave equation is the basis for most applications of the parabolic equation method, but the incoming wave equation is also required in the single-scattering solution. The parabolic equation method can be applied to seismo-acoustics problems, which involve both fluid and solid layers, by using the vector operators in Eq. (1) in solid layers, using a scalar operator in water layers, and enforcing interface conditions at fluid-solid interfaces.⁵

TABLE I. Elastic properties of the layers in example A, where c_p and c_s are compressional and shear wave speeds, ρ is density, and α_p and α_s are compressional and shear attenuations. The layers are numbered from the sea floor.

Example	Elastic layers	c_p (m/s)	c_s (m/s)	ρ (g/cm ³)	α_p (dB/λ)	α_s (dB/λ)
A	1	2400	1200	1.5	0.1	0.2
	2	4000	2500	3.0	1.0	2.0
	3	4000	2500	3.0	10.0	20.0

^{a)}Author to whom correspondence should be addressed. Present address: Boston University, Boston, Massachusetts. Electronic mail: jcollis@bu.edu

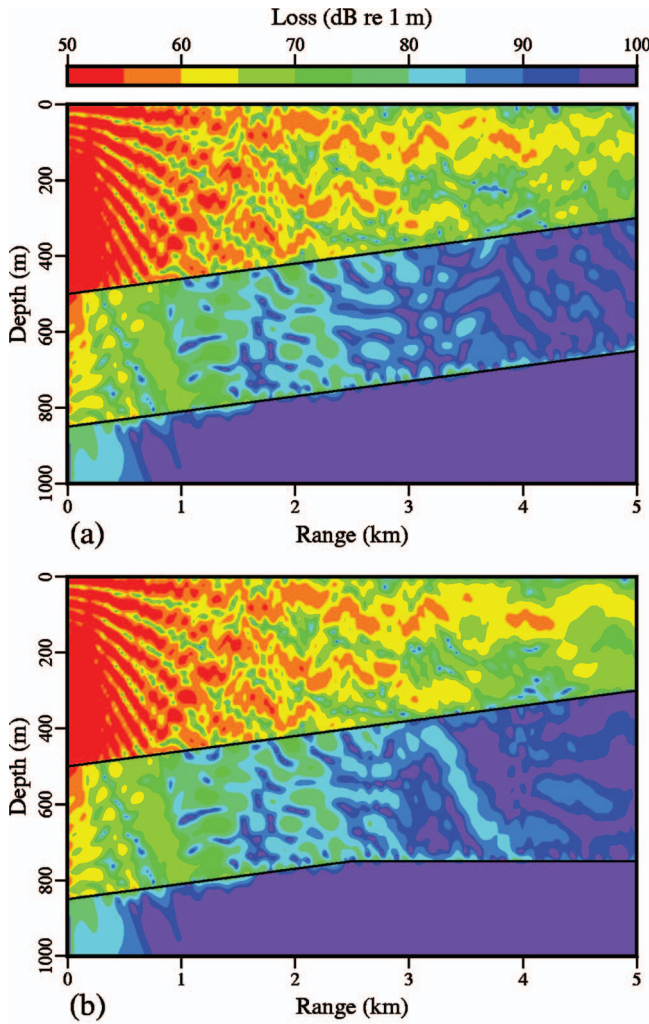


FIG. 1. Compressional transmission loss for Example A. For both cases, the sediment thickness is constant for $r > 2.5$ km. (a) The case in which sediment thickness remains constant for $r < 2.5$ km. (b) The case in which sediment thickness increases for $r > 2.5$ km.

The factorization that gives rise to the parabolic wave equations in Eq. (1) is based on the assumption that the medium is range independent. Range-dependent problems can be solved by approximating the medium in terms of a series

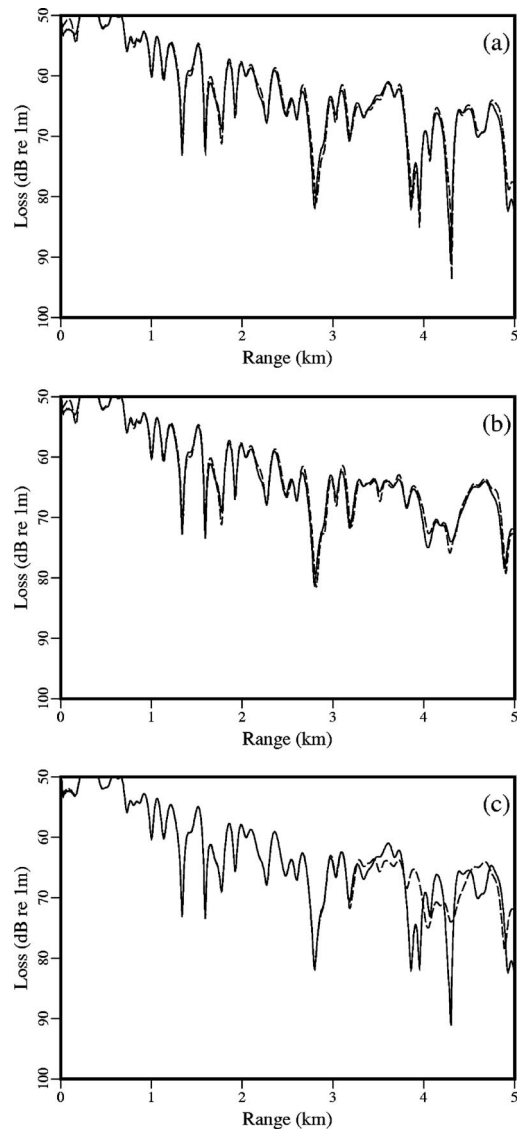


FIG. 2. Compressional transmission loss at $z=25$ m for example A. The dashed curves correspond to reference solutions that were generated using a finite-element model. The solid curves are the parabolic equation solutions for the cases of (a) constant layer thickness and (b) variable layer thickness. (c) Comparison between the parabolic equation solutions of the constant and variable layer thickness cases.

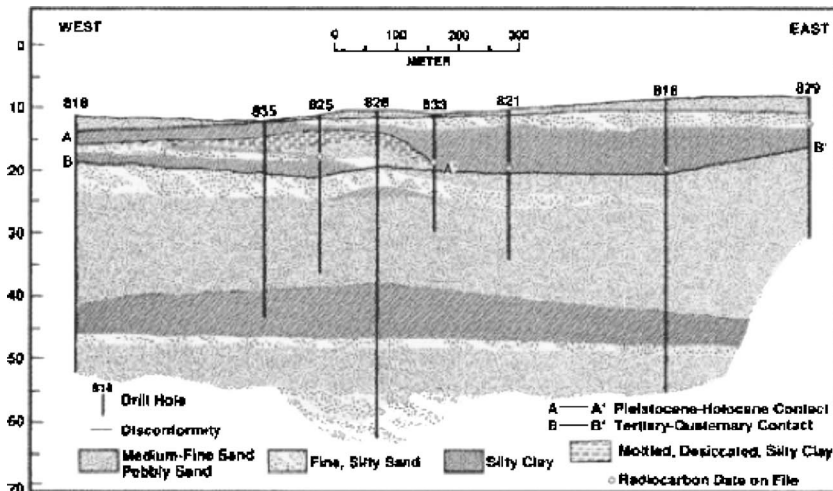


FIG. 3. The Atlantic Generating Site off the coast of New Jersey. Black vertical lines show boreholes where data were acquired and used to estimate the geoacoustic properties of layers. Image reused with permission from Badley *et al.* (Ref. 11) and the Acoustical Society of America.

TABLE II. Elastic properties of the layers in example B, where c_p and c_s are compressional and shear wave speeds, ρ is density, and α_p and α_s are compressional and shear attenuations. The layers are numbered from the sea floor.

Example	Elastic layers	c_p (m/s)	c_s (m/s)	ρ (g/cm ³)	α_p (dB/ λ)	α_s (dB/ λ)
B(1)	1	1800	872	2.08	0.24	1.0
B(2)	1	1733	817	2.0	0.37	1.37
	2	1866	927	2.15	0.11	0.63
B(4)	1	1733	817	2.0	0.37	1.37
	2	1997	1117	2.25	0.08	0.55
	3	1700	800	1.95	0.15	0.75
	4	1900	1000	2.15	0.1	0.6
B(8)	1	1900	850	2.3	0.05	0.55
	2	1600	700	1.7	1.0	3.0
	3	1700	900	2.0	0.05	0.55
	4	2100	1300	2.25	0.1	0.55
	5	1790	750	2.25	0.05	0.55
	6	2100	1300	2.25	0.1	0.55
	7	1700	800	1.95	0.15	0.75
	8	1900	1000	2.15	0.1	0.6

of range-independent regions and applying Eq. (1) to propagate the field through each region. For a purely solid medium, the vertical interfaces between range-independent regions can be handled by conserving the displacements and the stresses using the single-scattering solution, which is based on the equations

$$\begin{pmatrix} \sigma_{rr} \\ w \end{pmatrix} = R \begin{pmatrix} u_r \\ w \end{pmatrix}, \quad (2)$$

$$\frac{\partial}{\partial r} \begin{pmatrix} u \\ -\sigma_{rz} - \lambda_0 \frac{\partial u}{\partial z} \end{pmatrix} = S \begin{pmatrix} u_r \\ w \end{pmatrix}, \quad (3)$$

$$R = \begin{pmatrix} \lambda + 2\mu & \lambda \frac{\partial}{\partial z} \\ 0 & 1 \end{pmatrix}, \quad (4)$$

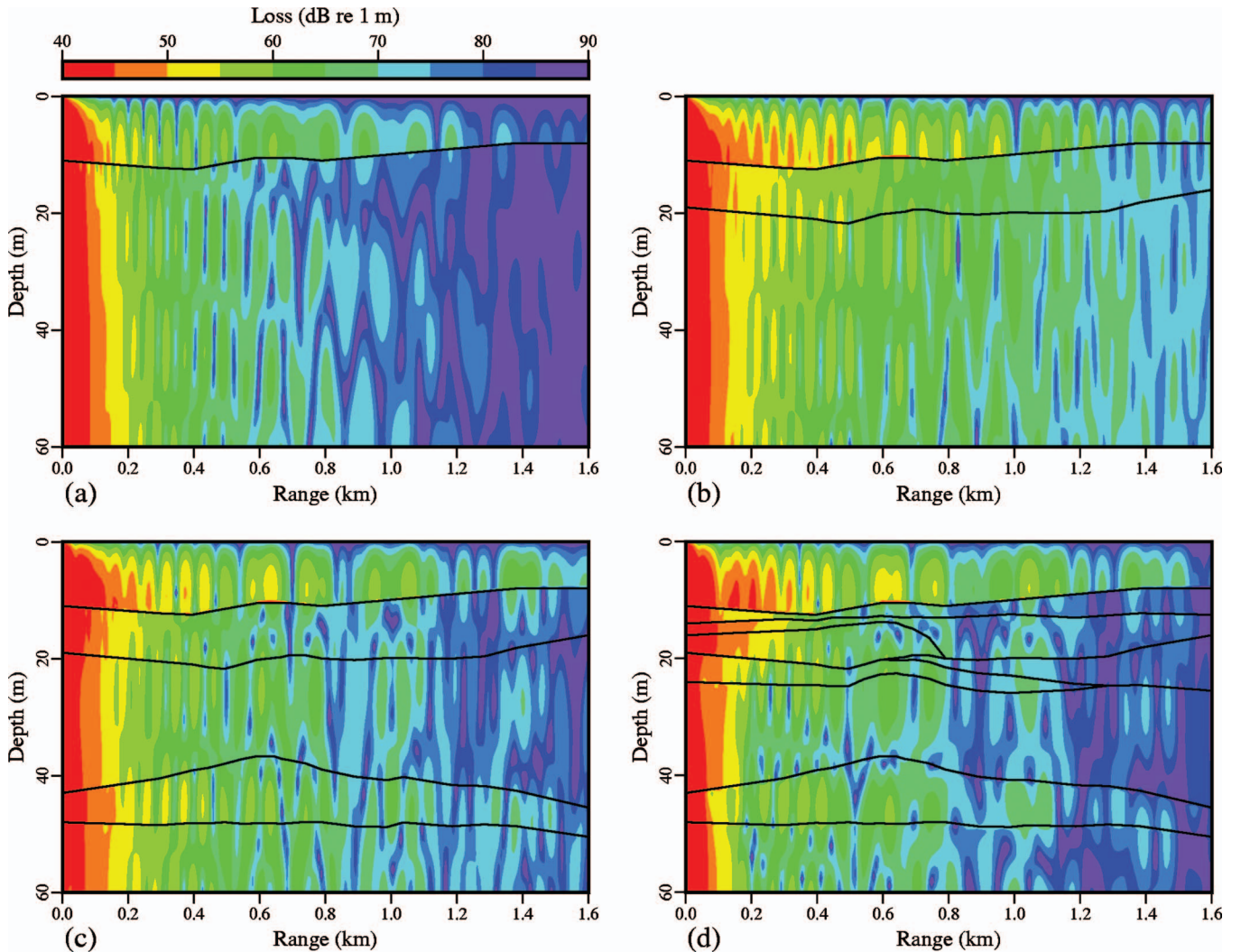


FIG. 4. Compressional transmission loss for example B. Approximations of the sediment structure based on (a) one, (b) two, (c) four, and (d) eight layers.

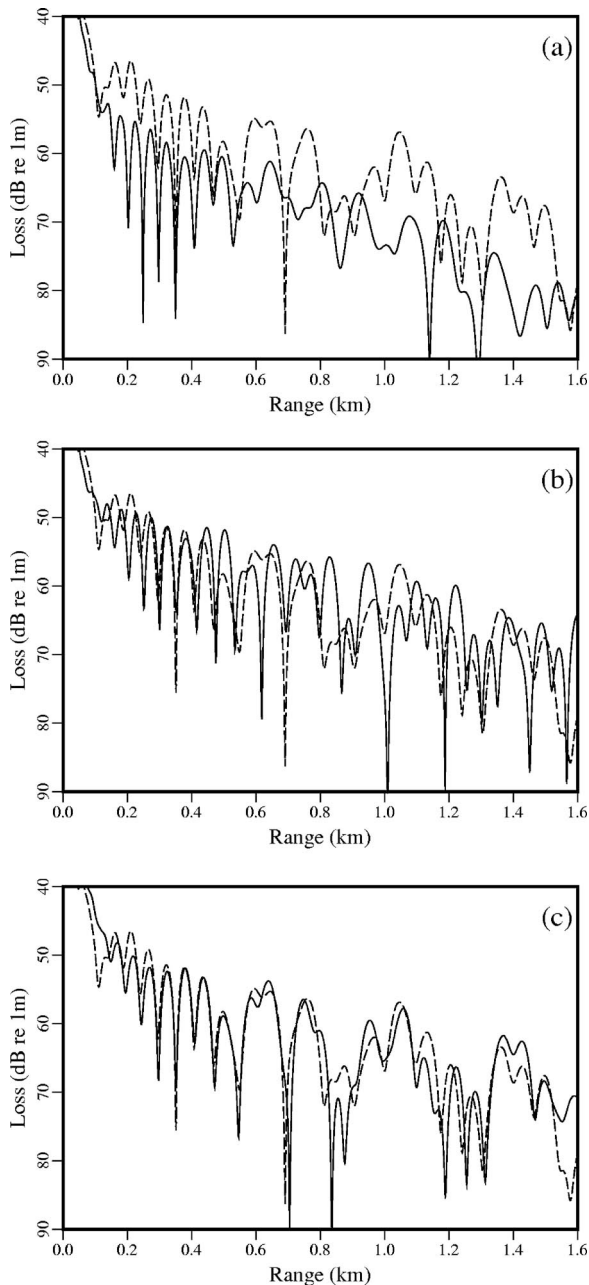


FIG. 5. Compressional transmission loss at $z=5$ m for example B. The dashed curve corresponds to the eight-layer solution. The solid curves correspond to the (a) one, (b) two, and (c) four layer approximations.

$$S = \begin{pmatrix} 1 & 0 \\ (\lambda - \lambda_0) \frac{\partial}{\partial z} + \frac{\partial \lambda}{\partial z} & \rho \omega^2 + \frac{\partial}{\partial z} (\lambda + 2\mu) \frac{\partial}{\partial z} \end{pmatrix}, \quad (5)$$

where λ and μ are the Lamé parameters, the constant λ_0 is a representative value of λ , and σ_{rr} and σ_{rz} are the normal and tangential stresses. The operators R and S relate the quantities that must be conserved across a vertical interface with the dependent variables.

Since σ_{rz} is conserved across both vertical and horizontal interfaces, an auxiliary condition has been added in Eq. (3) in order to avoid singular systems of equations. This condition is obtained by taking the depth derivative of the condition for conservation of u across the vertical interface,

which is valid since u is conserved at all depths along the vertical interface. The single-scattering solution is obtained by using the depth operators in Eq. (1) to eliminate the range derivative in Eq. (3) and obtaining an iteration formula for the reflected field in terms of the incident field. We apply a special case of the iteration formula that provides accurate solutions with only one iteration. After obtaining the reflected field, the transmitted field is then used as an initial condition in the next region.

The single-scattering solution is readily generalized to problems involving horizontal interfaces between fluid and solid layers. The condition for conservation of the acoustic pressure p is implemented as part of Eq. (2). The condition for conservation of the particle velocity $\partial p / \partial r$ is implemented as part of Eq. (3). A sloping fluid-solid interface at the ocean bottom is handled by rotating coordinates so that the range direction is tangent to the interface. The ocean bottom is approximated in terms of a series of constant slope regions. When a change in slope is encountered, the solution is propagated slightly beyond the change in slope in order to obtain an initial condition in the next region. The dependent variables are interpolated, extrapolated, and rotated as described in Ref. 8.

III. EXAMPLES

In this section, we apply the variable-rotated single-scattering solution to problems involving variations in bathymetry and layer thicknesses within an elastic bottom. We generate reference solutions using a finite-element model.¹⁰ For each of the examples, the sound speed is 1500 m/s in the water column, and an artificial absorbing layer is used to prevent reflections from the bottom of the computational grid.

For example A, the ocean depth is 500 m at the range of the source and slopes upward at approximately 2.3° . The sediment contains a layer over a half space and we consider two cases. In one case, the sediment thickness is 350 m for all r . In the other case, the sediment thickness is 350 m for $r < 2.5$ km and linearly increases to 450 m for $2.5 \text{ km} < r < 5$ km. Geoacoustic properties of the layers are given in Table I. A 25 Hz source is located at $z=390$ m. In the transmission loss plots appearing in Fig. 1, the significant differences in the water column at long ranges illustrate the influence of sediment thickness on the field. In the plots of transmission loss curves in Fig. 2, we observe that the parabolic equation solutions are in good agreement with the finite-element solution and once again note the differences in the solutions for the two cases.

For example B, we apply the parabolic equation model to a realistic environment involving multiple layers and complex stratigraphy that is based on borehole data from the Atlantic Generating Site (see Fig. 3) on the New Jersey Shelf.⁹ This shallow water site has been the location of broadband acoustic experiments over short range tracks.^{11–13} Geoacoustic properties of the layers are given in Table II. A 50 Hz source is located at $z=5$ m. For this problem, we consider a series of approximations of the sediment in terms of different numbers of layers. When thicker layers were

formed from multiple thinner layers, the properties were taken to be the average of the constituent layers. In order to test the importance of shear effects in such an environment, the shear speed values were chosen to be greater than those measured at the site. Compressional transmission loss is plotted for cases involving one, two, four, and eight layers in Fig. 4. The major differences between the one and two layer cases are mainly attributable to the fact that there is no interface within the sediment to reflect energy back into the water column in the one layer case, which results in a greater decay rate of amplitude with range. The two and four layer cases have similar amplitudes and are qualitatively similar. The four and eight layer cases are in fair quantitative agreement. The transmission loss curves appearing in Fig. 5 illustrate the differences between the cases more quantitatively.

IV. CONCLUSIONS

The variable rotated parabolic equation and the single-scattering method were combined to obtain an accurate and efficient approach for solving seismo-acoustics problems that involve variations in bathymetry and the thicknesses of elastic sediment layers. The accuracy of the model was demonstrated by making benchmark comparisons with solutions generated using a finite-element model. To illustrate that this parabolic equation solution is applicable to a large class of problems, we presented an example involving complex stratigraphy from the Atlantic Generating Site.

ACKNOWLEDGMENT

This work was supported by the Office of Naval Research, including an ONR Ocean Acoustics Graduate Traineeship Grant to the first author.

- ¹F. B. Jensen, W. A. Kuperman, M. B. Porter, and H. Schmidt, *Computational Ocean Acoustics* (American Institute of Physics, New York, 1994), pp. 343–412.
- ²R. R. Greene, “A high-angle one-way wave equation for seismic wave propagation along rough and sloping interfaces,” *J. Acoust. Soc. Am.* **77**, 1991–1998 (1985).
- ³M. D. Collins, “A higher-order parabolic equation for wave propagation in an ocean overlying an elastic bottom,” *J. Acoust. Soc. Am.* **86**, 1459–1464 (1989).
- ⁴B. T. R. Wetton and G. H. Brooke, “One-way wave equations for seismoacoustic propagation in elastic waveguides,” *J. Acoust. Soc. Am.* **87**, 624–632 (1990).
- ⁵M. D. Collins, “Higher-order Padé approximations for accurate and stable elastic parabolic equations with application to interface wave propagation,” *J. Acoust. Soc. Am.* **89**, 1050–1057 (1991).
- ⁶W. Jerzak, W. L. Siegmann, and M. D. Collins, “Modeling Rayleigh and Stoneley waves and other interface and boundary effects with the parabolic equation,” *J. Acoust. Soc. Am.* **117**, 3497–3503 (2005).
- ⁷E. T. Küsel, W. L. Siegmann, and M. D. Collins, “A single-scattering correction for large contrasts in elastic layers,” *J. Acoust. Soc. Am.* **121**, 808–813 (2007).
- ⁸D. A. Outing, W. L. Siegmann, M. D. Collins, and E. K. Westwood, “Generalization of the rotated parabolic equation to variable slopes,” *J. Acoust. Soc. Am.* **120**, 3534–3538 (2006).
- ⁹K. P. Bongiovanni, M. Badiéy, and W. L. Siegmann, “Shallow-water sediment layer structure and composition effects on range-dependent acoustic propagation at the Atlantic Generating Station (AGS) site,” *J. Acoust. Soc. Am.* **98**, 2249–2261 (1995).
- ¹⁰M. Zampolli, A. Tesei, F. B. Jensen, N. Malm, and J. B. Blottman, “A computationally efficient finite element model with perfectly matched layers applied to scattering from axially symmetric objects,” *J. Acoust. Soc. Am.* **122**, 1472–1485 (2007).
- ¹¹M. Badiéy, I. Jaya, and A.H.-D. Cheng, “Shallow water acoustic/geoacoustic experiments near the New Jersey Atlantic Generating Station site,” *J. Acoust. Soc. Am.* **96**, 3593–3604 (1994).
- ¹²M. Badiéy, K. P. Bongiovanni, and W. L. Siegmann, “Interpretation of frequency-dependent transmission-loss interference patterns,” *IEEE J. Ocean. Eng.* **22**, 219–225 (1997).
- ¹³M. Jaye, M. Badiéy, and W. L. Siegmann, “Geoacoustic profile estimation using empirical orthogonal functions for propagation applications,” *IEEE J. Ocean. Eng.* **26**, 795–808 (2001).